Atmospheric Environment 44 (2010) 3547–3557

Contents lists available at ScienceDirect

Atmospheric Environment

journal homepage: www.elsevier.com/locate/atmosenv

Source apportionment of airborne particulate matter in Southeast Texas using a source-oriented 3D air quality model

Hongliang Zhang, Qi Ying*

Zachry Department of Civil Engineering, Texas A&M University, College Station, TX 77843, USA

ARTICLE INFO

Article history:
Received 2 March 2010
Received in revised form
31 May 2010
Accepted 2 June 2010

Keywords:
Regional source apportionment
Primary particulate matter
Ammonium sulfate
AMS
TexAQS 2000

ABSTRACT

A nested version of the source-oriented externally mixed UCD/CIT model was developed to study the source contributions to airborne particulate matter (PM) during a two-week long air quality episode during the Texas 2000 Air Quality Study (TexAQS 2000). Contributions to primary PM and secondary ammonium sulfate in the Houston–Galveston Bay (HGB) and Beaumont–Port Arthur (BPA) areas were determined.

The predicted 24-h elemental carbon (EC), organic compounds (OC), sulfate, ammonium ion and primary $PM_{2.5}$ mass are in good agreement with filter-based observations. Predicted concentrations of hourly sulfate, ammonium ion, and primary OC from diesel and gasoline engines and biomass burning organic aerosol (BBOA) at La Porte, Texas agree well with measurements from an Aerodyne Aerosol Mass Spectrometer (AMS).

The UCD/CIT model predicts that EC is mainly from diesel engines and majority of the primary OC is from internal combustion engines and industrial sources. Open burning contributes large fractions of EC, OC and primary $PM_{2.5}$ mass. Road dust, internal combustion engines and industries are the major sources of primary $PM_{2.5}$. Wildfire dominates the contributions to all primary PM components in areas near the fires. The predicted source contributions to primary PM are in general agreement with results from a chemical mass balance (CMB) model. Discrepancy between the two models suggests that further investigations on the industrial PM emissions are necessary.

Secondary ammonium sulfate accounts for the majority of the secondary inorganic PM. Over 80% of the secondary sulfate in the 4 km domain is produced in upwind areas. Coal combustion is the largest source of sulfate. Ammonium ion is mainly from agriculture sources and contributions from gasoline vehicles are significant in urban areas.

1. Introduction

Southeast Texas is well known for the high density of industrial facilities located in the Houston–Galveston Bay (HGB) and Beaumont–Port Arthur (BPA) areas. Houston is the fourth-largest city in the United States with a population over 2.2 million. Based on the National Emissions Inventory (NEI) developed by the U.S. EPA, the emission rates of nitrogen oxides (NO_x), volatile organic compounds (VOCs) and fine particulate matter with aerodynamic diameter less than 2.5 μm ($PM_{2.5}$) from the HGB area are 27.4, 23.6 and 4.2 metric tons km^{-2} $year^{-1}$ in 2000, which exceed those from Los Angeles County in California (23.6, 21.4 and 3.0 tons km^{-2} $year^{-1}$, respectively). Because of the immense emissions of primary PM and precursors of secondary PM from both industrial and urban sources and the meteorology conditions characterized by high temperatures and intensive solar radiation as well as a land-sea breeze circulation that confines pollutants in Southeast Texas (Banta et al., 2005; Kleinman et al., 2002), HGB and BPA have possible difficulties meeting the national ambient air quality standards for $PM_{2.5}$ (Buzcu et al., 2006; Fraser et al., 2003; Nopmongcol et al., 2007). Quantitative knowledge of the contributions of different emissions sources to $PM_{2.5}$ concentrations is helpful to better understand $PM_{2.5}$ formation mechanisms and is crucial to the development of effective emission control strategies to reduce the adverse effects caused by $PM_{2.5}$ in HGB and BPA areas.

The receptor-oriented chemical mass balance (CMB) and positive matrix factorization (PMF) models are widely used tools to quantify source contributions to air pollutants. The total concentrations of each chemical species in ambient samples measured at receptor locations are reconstructed from a linear combination of emission source profiles (Watson et al., 2002). The CMB and PMF receptor models have been applied in many studies to determine

* Corresponding author. Tel.: +1 979 845 9709; fax: +1 979 862 1542.
E-mail address: qying@civil.tamu.edu (Q. Ying).

1352-2310/$ – see front matter © 2010 Elsevier Ltd. All rights reserved.
doi:10.1016/j.atmosenv.2010.06.004

the source contributions to PM in various parts of the country (Bullock et al., 2008; Lane et al., 2007; Robinson et al., 2006; Schauer and Cass, 2000; Zheng et al., 2002). In the HGB area, diesel and gasoline vehicles, road dusts, meat cooking operations and wood combustion have been identified as the main sources to primary $PM_{2.5}$ (Buzcu et al., 2006; Fraser et al., 2003). While the receptor models are robust and relatively easy to apply, they do not provide all the information needed to design effective control strategies. The fundamental non-reactive assumption in the model formulations limits their applications mainly to primary pollutants and they cannot be used to evaluate the effectiveness of different emissions control strategies. Because of the requirement of accurate PM chemical composition, they can only be used in locations where such detailed measurements are available. As an alternative method, source-oriented modeling approaches track emissions from different source categories and their physical and chemical transformations in mechanistic air quality models (Bhave et al., 2007; Wagstrom et al., 2008; Ying and Kleeman, 2006). The model results are then processed to generate source contribution estimations that cover the entire model domain. These models can also be used to evaluate different emissions control strategies.

The Texas 2000 Air Quality Study (TexAQS 2000) is a comprehensive campaign to improve understanding of the factors that control the formation and transport of air pollutants in Southeastern Texas. Previous regional modeling studies for the TexAQS 2000 episode were mainly focused on understanding high ozone formation (Byun et al., 2007; Nam et al., 2006; Vizuete et al., 2008) and only a few studies have been devoted to study PM (Nopmongcol et al., 2007). The regional source contributions to PM during this episode have not been determined.

In this study, the one-way nested source-oriented UCD/CIT air quality model was used to describe the emissions, transport, physical and chemical transformation and removal of airborne PM in southeast Texas during TexAQS 2000. The purpose of this study is to evaluate the performance of the UCD/CIT model in describing key gases and aerosol-phase pollutants and to determine the major sources that contribute to primary PM as well as secondary ammonium sulfate in the HGB and BPA areas during this episode. This work is a continuation of the development and application of the source-oriented UCD/CIT model and represents the first application of the model in a geographical region outside California. Source contributions to secondary organic aerosol are not considered and will be evaluated in a separate study.

2. Model description

The UCD/CIT source-oriented air quality model has been applied and evaluated in several previous studies on source apportionment of PM and visibility impairment in the South Coast Air Basin and the Central Valley of California (for example, see Chen et al., 2009; Kleeman and Cass, 2001; Ying and Kleeman, 2006; Ying et al., 2009). Details of the model development history and underlying principles have been described elsewhere (Ying et al., 2008a, 2008b, and the references therein), so only a brief summary is given below along with descriptions of recent updates to the model.

The UCD/CIT model can be used to directly determine the source contributions to both primary and secondary PM. The gas phase mechanism was expanded to predict the formation as well as the source origin of semi-volatile compounds by tracking the emission and transformation of reactive precursors and intermediate products from different sources. In this study, emissions of NO_x, sulfur dioxide (SO_2) and ammonia (NH_3) from different sources and their reaction products (for example, N_2O_5, HNO_3, H_2SO_4, etc.) are independently simulated in the model by attaching source tags to species from different sources. To determine the contributions to secondary PM, the representation of particle species is expanded to allow direct tracking of the gas-to-particle partitioning of the tagged precursor gases from different sources. This enables the model to determine the source contributions to nitrate (NO_3^-), ammonium (NH_4^+), and sulfate (SO_4^{2-}) in this study. The UCD/CIT model can be configured as to use an externally mixed particle representation to directly determine the source contributions to primary PM (Kleeman et al., 1997). In this study, the particles are represented as internally mixed aerosols and an artificial tracer approach is used to determine source contributions to primary PM (Ying et al., 2008b).

The original source-oriented UCD/CIT model is revised to include a one-way nested domain capability that allows the nested domains to use tagged boundary conditions for each emission source category based on source contribution results from a parent domain. This modification allows a more complete source attribution of PM by directly resolving the contributions from different upwind sources to concentrations in the nested domain. This is especially important when the contributions from upwind sources are significant compared to the sources within the nested domain. The original chemical mechanism used in the UCD/CIT model was a revised version of the SAPRC-90 mechanism (Carter, 1990). The SAPRC mechanism in this version of the UCD/CIT model is updated to a revised SAPRC-99 mechanism. An automatic mechanism generator was developed to create source-oriented SAPRC chemical mechanism that treats the reactions of species from different sources separately. The particle dry deposition scheme is updated in this version of the UCD/CIT model so that dry deposition velocities of particles are land cover and season dependent (Gong et al., 2003; Zhang et al., 2001).

3. Model application

3.1. Domain setup and meteorology inputs

In this study, the nested version of the UCD/CIT model is applied to simulate the air quality in eastern Texas during a two-week long (August 24, 2000–September 5, 2000) air quality episode in the TexAQS 2000 study. The horizontal grid sizes for the three nested domains are 36 km, 12 km and 4 km, respectively. The number of horizontal grid cells for these domains are 62×67, 89×89, and 83×65, respectively. A diagram that shows the position of the nested domains can be found in Fig. S1(a) of the Supplementary materials. The stations used in the analysis are shown on Fig. S1 (b), and a station list table can be found in Table S1. 14 vertical layers that reach approximately 15 km above surface are used. The first layer height is approximately 42 m. The detailed vertical grid information is included in Table S2 of the Supplementary materials. All three domains use the same vertical layer setup.

In this study, the meteorology fields were generated using the PSU/NCAR mesoscale model (MM5) by the Texas Commission of Environmental Quality (TCEQ) and were converted into the data format required by the UCD/CIT model using a preprocessing program. The reaction rate constants for photolysis reactions were calculated off-line with the JPROC preprocessing program distributed with the Community Multiscale Air Quality (CMAQ) model version 4.6 (Byun and Schere, 2006). Adjustments of the photolysis rate due to cloud cover are calculated based on the algorithm described in Byun and Ching (1999).

3.2. Emission inputs

Emissions of gaseous and particulate matter for the source-oriented UCD/CIT model were based on the 2001 Clean Air Interstate Rule (CAIR) emission inventory. Emissions from wildfire during the modeling episode were based on the data provided from the Center

for Energy and Environmental Resources at the University of Texas at Austin. Continuous Emission Monitoring (CEM) data were used to replace annual emission data for electricity generation utilities. The revised emission inventory was processed using a revised SMOKE (Sparse Matrix Operator Kernel Emissions) model version 2.4. Biogenic emissions were generated using the Biogenic Emissions Inventory System, Version 3 (BEIS3) included in the SMOKE distribution. The 1-km resolution BELD3 and cover data with 230 different cover types (Vukovich and Pierce, 2002) were used to estimate emissions from vegetation and soil.

Modifications were made to the original SMOKE program to generate emissions for each emission category using a sub-set of the emission inventory data determined by a list of Source Classification Codes (SCCs) for that emission source category. An SCC filter is added to the SMOKE program so that the program only processes the emission inventory data listed in SCC code list. Nine primary PM emission categories (mobile gasoline engines, mobile diesel engines, high sulfur fuel (boilers, engines and industrial processes using oil or natural gas), wildfire, open burning (including household cooking, waste disposal and agriculture burning), road dust, agriculture dust, sea salt and other sources) and eight gas emission categories (diesel engines, gasoline engines, oil and gas production, high sulfur fuel, coal combustion, fire (including wildfire and open burning), biogenic, and other sources) were used in generating the emissions.

Table 1 lists the daily emission rates of gas phase precursors of secondary inorganic aerosol for all the emission source categories for August 31, 2000, a typical weekday with significant wildfire activities. Coal combustion accounts for the majority of the SO_2 emissions. Table 2 lists the daily emission rates of $PM_{2.5}$ elemental carbon (EC), organic compounds (OC), nitrate, sulfate and other components. Diesel vehicles and open burning are the two largest anthropogenic sources of EC. Approximately 47% of primary OC and 40% of primary $PM_{2.5}$ mass (less wildfire) are emitted from the "other" sources, while diesel and gasoline engines combined only account for 16.7% and 11.1% of primary OC and $PM_{2.5}$ mass, respectively. Analysis of the emission inventory shows that approximately 60% of the primary $PM_{2.5}$ in the "other" source category is from industrial point sources (mainly catalyst cracking, process heaters and furnace electrode manufacture) and 40% is from area sources (mainly road construction and commercial charbroiling).

The UCD/CIT uses sectional representation of particle size distributions with 15 size bins that cover the size range of 0.001–10 μm for the primary emitted particles. Modifications were made to the SMOKE program to generate size resolved PM emissions. The $PM_{2.5}$ speciation profiles included in the auxiliary data of the 2001 CAIR emission inventory were expanded to generate size- and composition-resolved source profiles using particle size and composition distribution information collected from various data sources described below. Detailed particulate emission size distributions measurements of mass and major chemical components are available for diesel and gasoline engines (Kleeman et al., 2000), residential wood burning, meat cooking and cigarette smoking (Kleeman et al., 1999) and open burning of agriculture mass (Hays et al., 2005). Several data sources contain particle size distribution of mass but not chemical components so it is assumed that all chemical species will have the same size distribution as the reported mass distribution. These profiles include feedlot dust (Sweeten et al., 1998), road dust (Wang et al., 2005), tire wear (Kupiainen et al., 2005) and locomotive emissions (Fritz, 2000). For other sources without explicit size resolved measurements, rough estimation of the size distributions was made based on the 3-sizebin data from Taback et al. (1979). Sea salt emissions from wave breaking were generated based on the algorithm described in Zhang et al. (2005a) and Lewis and Schwartz (2006).

Table 1
Daily emission rates of gas phase precursors for each source on August 31, 2000 in the 4 km model domain. (Units: kmol day^{-1}).

Source types	NO	NO_2	SO_2	NH_3
Diesel	1224.7	64.4	73.1	4.0
Gasoline	693.7	36.4	19.4	139.7
Oil/gas production	184.0	9.7	0.4	0.0
High sulfur fuel	8665.6	455.8	951.1	90.0
Coal combustion	2197.1	115.6	4231.8	1.3
Open burning and wildfire	709.2	37.4	1.1[a]	327.2
Other	4429.8	233.0	4156.6	1648.8
Biogenic	1083.6	0.0	0.0	0.0
Total	19 187.3	952.2	9433.1	2210.8

[a] Emissions of SO_2 from wildfire were not considered in this study.

Table 2
Daily emission rates of sulfate, nitrate, EC, OC, other components and $PM_{2.5}$ mass for each source on August 31, 2000 in the 4 km model domain. (Units: kg day^{-1}).

Source types	Sulfate	Nitrate	EC	OC	Other	$PM_{2.5}$
Diesel	260.5	21.2	9650.4	2944.5	99.0	12 975.6
Gasoline	105.9	17.7	742.9	3391.9	842.6	5100.9
High sulfur fuel	1343.5	28.4	123.8	3008.1	1333.1	5836.9
Open burning	649.6	60.7	2096.8	6884.8	13 064.0	22 755.9
Road dust	50.0	43.1	196.1	2662.0	39 826.0	42 777.1
Agriculture dust	3.1	8.7	29.6	435.6	7514.7	7991.7
Other	8238.6	186.2	2246.6	18 694.9	35 293.2	64 659.6
Wildfire	1545.2	153.7	12 360.9	59 490.0	3708.5	77 258.4
Sea salt	30.6	14.5	0.0	0.0	0.0	384.7
Total	12 227.0	534.2	27 447.2	97 511.7	101 681.0	239 740.8

4. Results and discussion

4.1. Model performance evaluation

The predicted concentrations of gaseous and PM species in the 4 km domain were compared with surface observation data. In general, predicted concentrations of O_3, NO_x and CO agree well with observations. SO_2 concentrations at industrial sites are slightly over-predicted. Peak O_3 concentrations are under-predicted at several stations due to underestimation of the high reactive VOC emissions from industrial sources (Nam et al., 2006; Vizuete et al., 2008; Ying and Krishnan, 2010). This underestimation of O_3 does not affect the primary PM source apportionment results but may lead to some underestimation of local secondary sulfate concentrations. The following analyses are focused on evaluating the overall model performance on PM predictions. Complete time series of gaseous and PM species are included in the Supplementary materials (Figs. S2–S10).

Fig. 1 shows the mean fractional bias (MFB) and mean fractional error (MFE) for $PM_{2.5}$ EC, OC, sulfate, ammonium ion and mass based on the daily averaged species concentrations across different stations. The definitions of MFB and MFE are shown in equations (1) and (2):

$$\mathrm{MFB} = \frac{1}{N}\sum_{i=1}^{N}\frac{C_m - C_o}{(C_m + C_o)/2} \quad (1)$$

$$\mathrm{MFE} = \frac{1}{N}\sum_{i=1}^{N}\frac{|C_m - C_o|}{(C_m + C_o)/2} \quad (2)$$

where C_m is the model-predicted concentration at station i, C_o is the observed concentration at station i, and N equals the number of

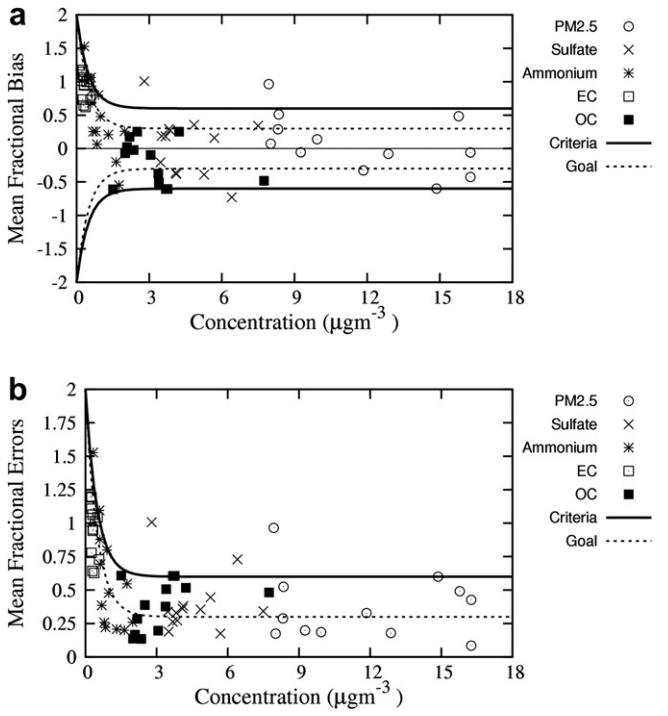

Fig. 1. Mean fractional bias (a) and errors (b) for $PM_{2.5}$ mass, sulfate, ammonium, EC and OC along with the proposed performance goals and criteria that vary as a function of species concentration. One $PM_{2.5}$ data point (concentration = 25.6 μg m^{-3}, MFB = 0.06, MFE = 0.13) is not shown on the plots.

prediction–observation pairs drawn from all monitoring stations. The lines on the figure show the suggested performance goals (solid lines) and criteria (dash lines) as a function of observed concentration. Performance goals are the level of accuracy that is close to the best a model can be expected to achieve and performance criteria are the level of accuracy that is acceptable for standard modeling applications (Boylan and Russell, 2006). The observation data used in the calculation were from 6 stations that cover urban, industrial and suburban locations (BAYP, CONR, DRPK, GALC, HALC and JEFC, see Fig. S1). The analysis includes 13 days of data from August 24, 2000 to September 5, 2000. Most species meet their individual performance criteria. Sulfate ion meets the criteria for 11 out of 13 days for both MFB and MFE. The total primary $PM_{2.5}$ meets the criteria for 12 out of 13 days for both MFB and MFE. All EC and OC predictions are within the model performance criteria. Over 50% of the data points are within the model performance goal.

Fig. 2 shows the comparison of predicted $PM_{2.5}$ sulfate, nitrate and primary OC concentrations and the observed concentrations by an Aerodyne Aerosol Mass Spectrometer (AMS) at La Porte (LAPT). The AMS results were provided in 10 or 15-min time resolution and were averaged to 1-h to compare with the model predictions. More details about the AMS measurements at LAPT can be found in Wood et al. (2010) and the references therein. The predicted and observed sulfate concentrations are on the same order of magnitude as the AMS, and the predicted diurnal and episode trends show general good agreement with the observations. Predicted low nitrate concentrations of approximately 0.5 μg m^{-3} at LAPT are at same level as the AMS measurements although the diurnal variation is not well captured by the model on a few days. Panel 2(c) shows the BBOA (biomass burning-like organic aerosol) based on the AMS data and the predicted other primary OC by the UCD/CIT model. The dashed line shows the contributions from predicted open burning and wildfire sources and the solid line shows the contributions from open burning, wildfire and other sources. The predicted

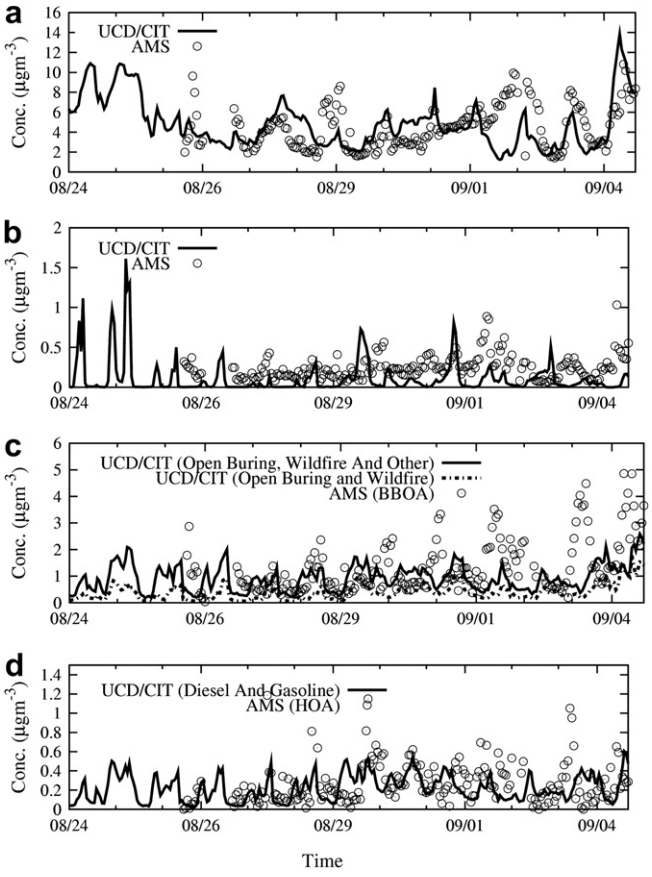

Fig. 2. Time series of concentrations of $PM_{2.5}$ sulfate (a), nitrate (b), primary organic compounds from biomass burning (c) and diesel and gasoline engines (d) predicted by the UCD/CIT model (lines) and measured by an AMS (open circles) between August 24and September 5, 2000.

biomass burning (open burning and wildfire) alone does not fully explain the BBOA from AMS. Including primary OC from other sources improves the agreement between the observations and predictions but the high concentrations of BBOA on September 2, 3 and 5 are not reproduced. This is likely due to incompleteness in the wildfire emission inventory. Panel 2(d) shows the HOA (hydrocarbon-like organic aerosol) from AMS and the predicted primary OC from diesel and gasoline vehicle sources. HOA from AMS data have been considered as mostly due to primary organic aerosols from diesel and gasoline combustions (Zhang et al., 2005b) and thus allow a direct comparison with the UCD/CIT results. The predicted concentrations of primary OC from diesel and gasoline engines combined are in the range of 0–0.5 μg m^{-3}, which agree well with the AMS measurements. There is no significant episode trend in the observed and predicted concentrations and the diurnal variations are generally well reproduced by the model (Fig. 3).

4.2. Comparison with CMB results

The predicted primary PM source apportionment results were compared with the results from an independent CMB source apportionment study that uses organic tracers and 3 inorganic elements to resolve contributions of gasoline vehicles, diesel vehicles, vegetative detritus, meat cooking, wood burning, and road dust to $PM_{2.5}$ OC and mass at three stations (LAPT, HRM3 and HALC). More details about the CMB study can be found in Buzcu et al. (2006). The UCD/CIT model does not have explicit vegetation detritus and meat cooking sources so the predicted contributions

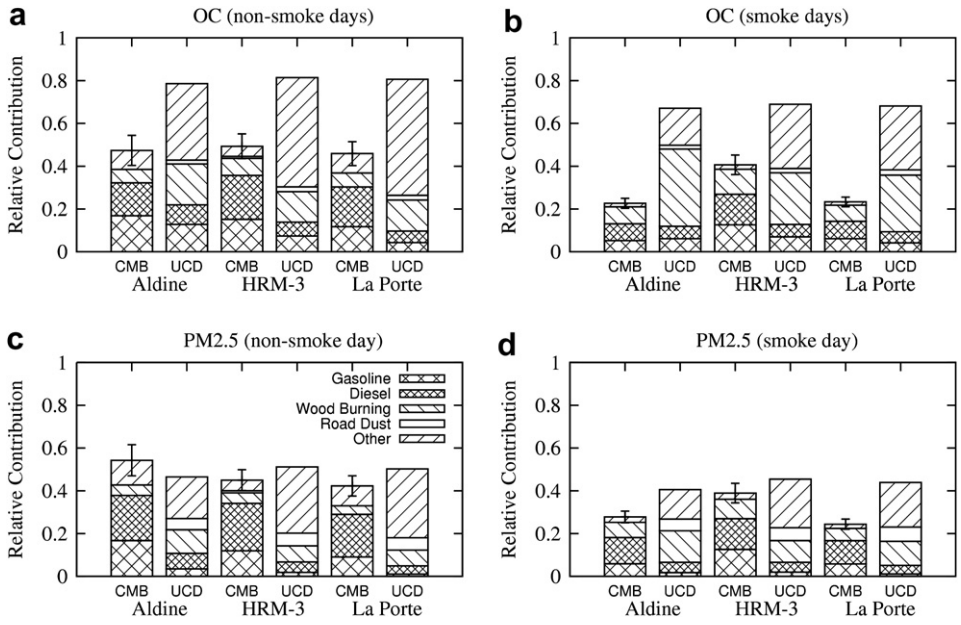

Fig. 3. Relative source contributions of primary $PM_{2.5}$ OC and mass concentrations to total $PM_{2.5}$ OC and mass predicted by a CMB receptor model and the UCD/CIT source-oriented air quality model at Aldine, HRM-3 and La Porte.

from these two sources by the CMB model are lumped into the "other" sources in the comparison. The open burning and wildfire contributions from the UCD/CIT model are combined to compare with the wood burning contributions from CMB. Since open burning contains not only wood combustion but also other types of burnings, this combination may slightly over estimate the actual wood burning contributions.

The CMB analyses were performed for two groups of $PM_{2.5}$ speciation data. One group contains the averaged concentrations for non-smoke days when wildfire influence was small (August 15, 21 and 27, 2000) and the other dataset for smoke days (September 2, 14, 20 and 30, 2000). Since the current model episode covers only part of the CMB dataset, averaged results from August 24–27, 2000 were used to compare with the non-smoke day CMB results and results from September 3–5, 2000 were used to compare with the smoke day CMB results. The relative contributions of each source from the CMB analysis are based on the apportioned primary OC and $PM_{2.5}$ mass from each source and the measured $PM_{2.5}$ OC and mass (including secondary PM) reported in Tables 2 and 3 of Buzcu et al. (2006). Relative contributions predicted by the UCD/CIT model are based on the predicted primary OC and $PM_{2.5}$ mass and overall $PM_{2.5}$ OC and mass with secondary components.

Panels 3(a) and (b) show the comparison of primary source contributions to OC for non-smoke and smoke days, respectively. The UCD/CIT model predicts a much higher primary OC fraction (60–80%) in total OC due to possible under-prediction of secondary organic aerosol (Chen et al., 2010; Kleeman et al., 2007). On the other hand, the CMB might slightly under-predict the primary OC from other sources, as some of the CMB reconstructed tracer concentrations are much lower than measurements (see Fig. 5 of Buzcu et al., 2006). Both models show significant diesel and gasoline engines contributions but the UCD/CIT model predicts higher contributions from wood smoke. The UCD/CIT model also predicts larger contributions from the "other" sources. Both models show a slight decrease in primary OC fraction and an increase of OC from wildfire that rivals the contributions from diesel and gasoline engines on smoke days. The predicted contributions from gasoline, diesel and wildfire contributions by the two models agree much better on the smoke days. Panels 3(c) and (d) show the relative contributions of primary $PM_{2.5}$ sources to total $PM_{2.5}$ on non-smoke and smoke days, respectively. The models agree well that approximately 50% of $PM_{2.5}$ was primary on non-smoke days and 30–40% on smoke days. The decrease of primary fraction is due to

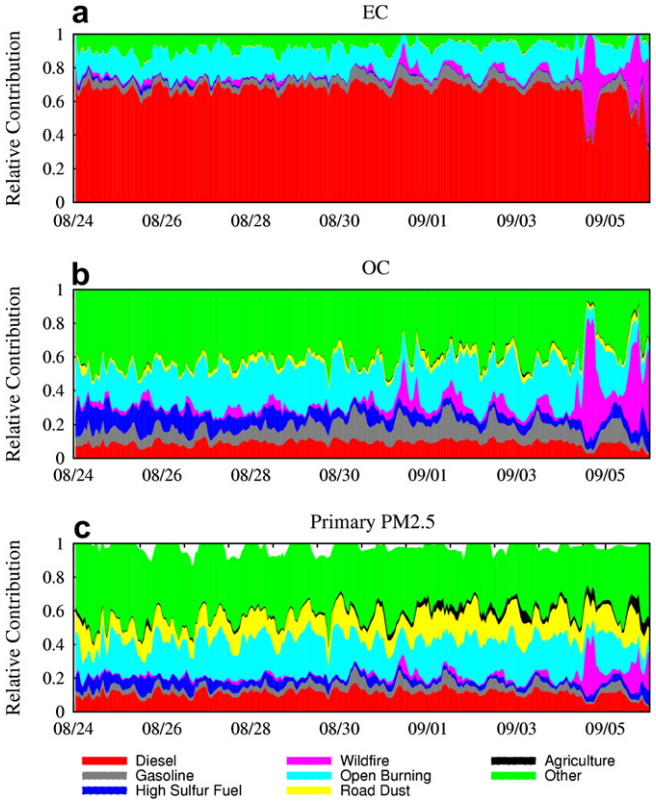

Fig. 4. Relative source contributions to primary $PM_{2.5}$ EC (a), OC (b), and mass (c) at Deer Park (DRPK) from August 24, 2000 to September 5, 2000. The "Other" category for EC and OC includes contributions from upwind sources. Contributions from upwind sources for primary $PM_{2.5}$ are explicitly represented by the white space on Panel (c).

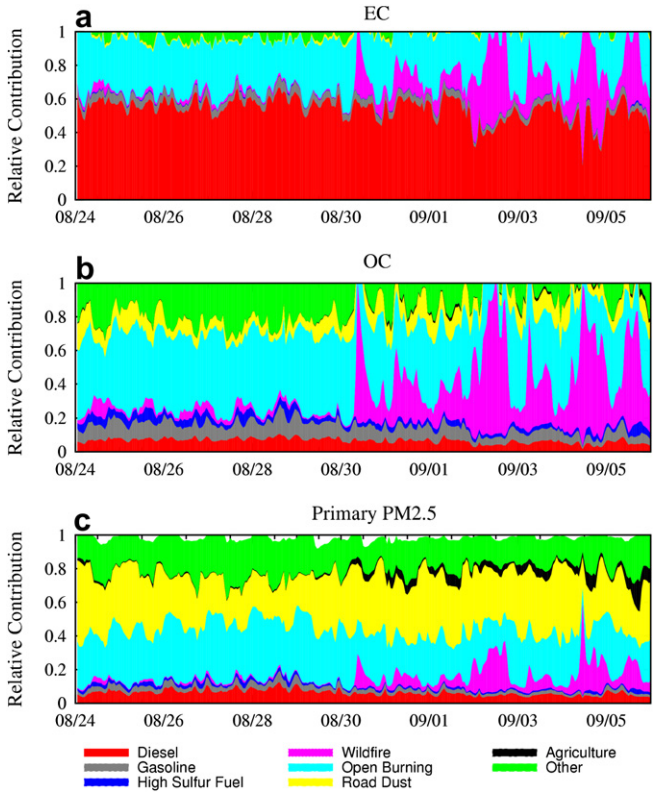

Fig. 5. Relative source contributions to primary $PM_{2.5}$ EC (a), OC (b), and mass (c) at Conroe (CONR) from August 24, 2000 to September 5, 2000. The "Other" category for EC and OC includes contributions from upwind sources. Contributions from upwind sources for primary $PM_{2.5}$ are explicitly represented by the white space on Panel (c).

significant regional transport of secondary sulfate into the model domain on the smoke days selected for this analysis (see Fig. 9). Both models predict higher contributions from diesel engines to the total $PM_{2.5}$ than gasoline engines. However, the UCD/CIT model again predicts higher contributions from the "other sources" and wood smoke sources and lower contributions from diesel and gasoline engines.

The emissions data in Table 2 suggest that approximately 40% of primary $PM_{2.5}$ (excluding wildfire) in the 4 km model domain is from the "other" sources. Analysis of the emission inventory shows that approximately 60% of the primary $PM_{2.5}$ in the "other" source category is from industrial point sources (mainly catalyst cracking, process heaters and furnace electrode manufacture) and 40% is from area sources (mainly road construction and commercial charbroiling). Thus, the UCD/CIT model results of significant contributions from the "other" sources are consistent with emission inventory data. The UCD/CIT model-predicted OC from diesel and gasoline engines seems to agree well with the AMS data, suggesting that the PM emissions from these two sources are generally well represented in the emission inventory. Previous studies showed significant contributions to VOCs in the HGB area from industrial sources (De Gouw et al., 2009; Wert et al., 2003) so it is expected that they should also contribute to the observed PM concentrations. However, few other independent studies of PM exist so additional analysis is necessary to validate the PM emission inventory regarding emissions from other sources, especially from industrial sources.

4.3. Source apportionment of primary particulate matter

The internally mixed UCD/CIT model tracks total primary particulate matter from different emission sources using non-reactive tracers for primary mass emissions. Contributions from all local sources, including the lumped group "other", can be directly determined based on the tracer concentrations. However, some of the particles from upwind locations also contribute to the primary $PM_{2.5}$ mass.

The EC and OC concentrations from each source are calculated based on the primary $PM_{2.5}$ and the corresponding source profile. However, it is difficult to directly predict EC and OC contributions from "other" sources as it is impossible to use a single source profile to represent all the sources that are included in the "other" category. Instead, the contributions from "other" sources to EC and OC were calculated based on the difference of the predicted total EC and OC and the calculated EC and OC from all explicit sources. Thus, the resulting "other" EC and OC include contributions from boundary conditions in addition to all other local sources.

Fig. 4 shows the predicted hourly-averaged relative source contributions to $PM_{2.5}$ EC, OC and primary $PM_{2.5}$ mass at DRPK from sources within the 4 km domain during the study period. The DRPK site is located east of the Houston urban center and is close to the Houston Ship Channel. Contributions to EC at DRPK are mainly from diesel engines (approximately 70%) and open burning

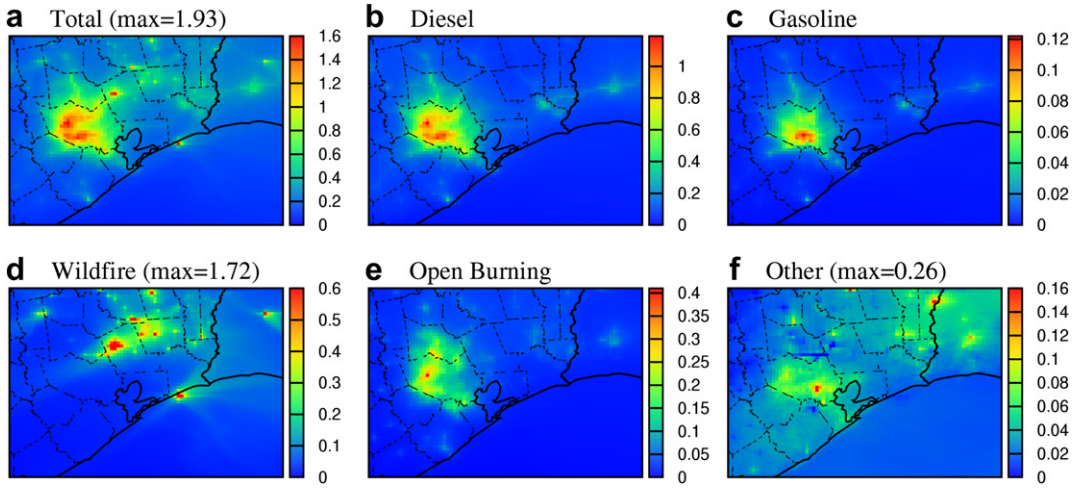

Fig. 6. Episode-averaged source contributions to $PM_{2.5}$ EC concentrations. The scale on each panel is different. Units are μg m^{-3}. The scales of a, d, and f are adjusted to show better spatial distribution and the maximum values are shown with the titles.

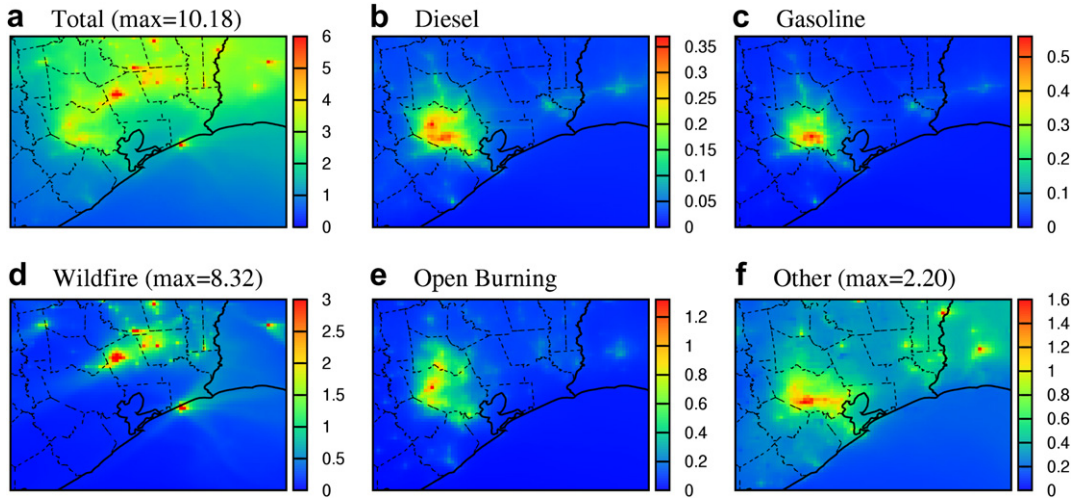

Fig. 7. Episode-averaged source contributions to OC concentrations. The scale on each panel is different. Units are μg m^{-3}. The scales of a, d, and f are adjusted to show better spatial distribution and the maximum values are shown with the titles.

(approximately 20%). Contribution from wildfire increases on September 4–5, 2000, with a maximum contribution of approximately 50%. The contributions of gasoline engines and road dust to EC concentrations are small.

Panel 4(b) shows that diesel and gasoline engines combined contribute to approximately 20% of the primary OC, with approximately equal contribution from each source. The diurnal variation in the gasoline contributions is more significant than that of diesel engines. Approximately 20–30% of the OC originate from open burning and 5–10% from high sulfur fuel. Contributions from road dust to primary OC are small. Other OC sources account for about 40–55%. A further check of the emission data shows that approximately 70% of the OC in the "other" source category are from industrial sources. The contribution from wildfire increases from almost zero to about 80% in September 4–5, 2000.

Panel 4(c) shows the relative contributions to primary $PM_{2.5}$ mass. Open burning accounts for approximately 20% of the primary $PM_{2.5}$. Contributions from diesel engines are about 15–20%. Road dust is another important source of primary $PM_{2.5}$ with relative contributions of 10–20%. Contributions from gasoline engines and high sulfur fuel to primary $PM_{2.5}$vary between 5 and 10%. Wildfire contributions peak at approximately 30% in the last few days of the study episode. Large contributions from other sources are likely due to industrial sources, based on an analysis of the emission inventory.

Fig. 5 shows the source contributions to $PM_{2.5}$ EC, OC and mass concentrations at CONR. The CONR site is situated in an urban

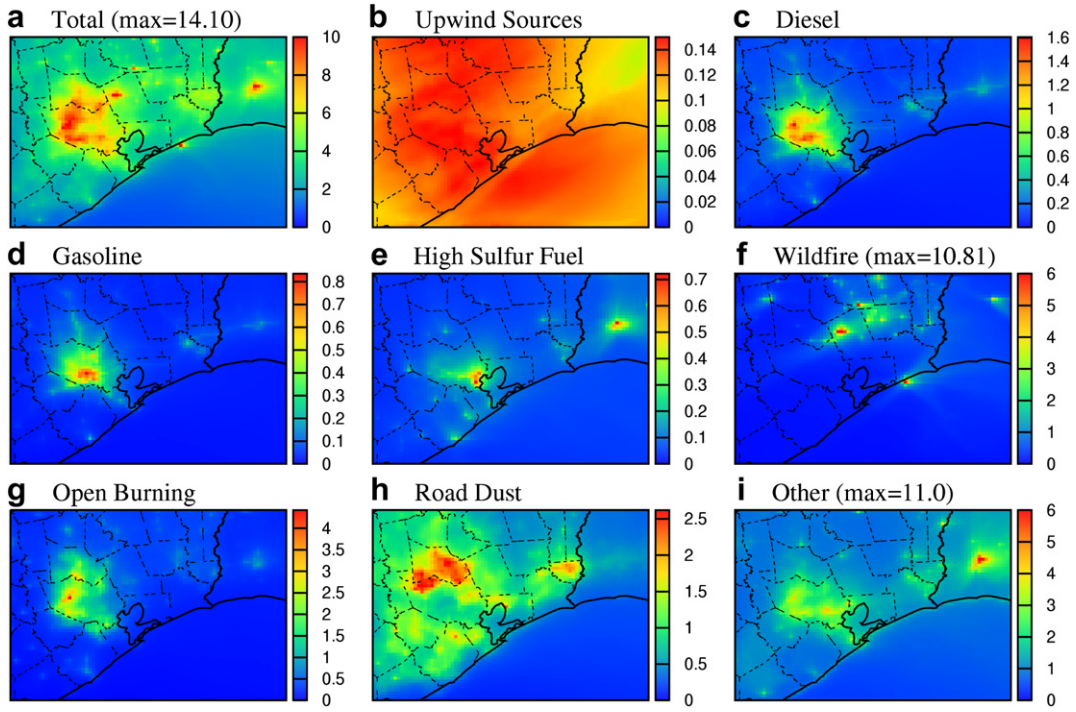

Fig. 8. Episode-averaged source contributions to primary $PM_{2.5}$ mass concentrations. The scale on each panel is different. Units are μg m^{-3}. The scales of a, f, and i are adjusted to show better spatial distribution and the maximum values are shown with the titles.

commercial area approximately 40 miles north of Houston, away from major industrial emissions. Panel 5(a) shows that 50–60% EC is from diesel engines. Open burning is the second largest source with relative contributions of approximately 30%. Wildfire contributes to about 50% in the last few days. The combined contributions of road dust, gasoline engines and high sulfur fuel to EC are less than 10%.

Panel 5(b) shows that diesel and gasoline engines account for less than 20% of OC at CONR. The relative contribution from road dust is approximately 5%. Contribution from open burning accounts for about 40% of the total OC. Contributions of other sources are approximately 10–20% throughout the episode. OC from wildfire dominates the last few days with relative contributions as high as 100% on some hours.

Panel 5(c) describes the relative source contributions to primary $PM_{2.5}$ mass at CONR. Open burning and road dust are two main sources and account for approximately 60% of the predicted $PM_{2.5}$ mass concentrations during the entire episode. $PM_{2.5}$ from diesel vehicles is less than 10%. The contribution from wildfire to primary $PM_{2.5}$ mass increases to approximately 25% on September 2, 2000 and even reached approximately 50% on September 4, 2000. Contributions of gasoline vehicles and high sulfur fuel sources are negligible and contributions from other sources are about 20%.

Fig. 6 shows the regional source contributions to episode average $PM_{2.5}$ EC concentrations. The minimum to maximum value scale is used for all the regional figures in this section. To better show the spatial distribution, the maximum values of the scale of some figures are adjusted with the maximum values attached with titles. Panel 6(a) shows that high EC concentrations occur in the Houston urban areas with a maximum concentration of 1.93 $\mu g\ m^{-3}$. As shown in Panel 6 (b), the dominant source of EC in the urban area is diesel engines which account for approximately 60% of total EC. In addition to diesel vehicles, diesel-powered construction equipment is an important source of diesel emissions. This explains the wider spatial distribution of diesel engine contributions than gasoline engine contributions. Contribution from gasoline engines is also highest in the urban area with a maximum contribution of 0.12 $\mu g\ m^{-3}$ as shown in Panel 6(c). Wildfire dominates local EC concentration with a highest contribution of 1.73 $\mu g\ m^{-3}$. Open burning also has wide spatial distribution around the Houston area. All other anthropogenic sources combined contribute to approximately 0.20 $\mu g\ m^{-3}$ near the Houston Ship Channel and approximately 0.15 $\mu g\ m^{-3}$ in the BPA area.

Fig. 7 shows the predicted source contributions of episode average primary OC from August 24, 2000 to September, 5, 2000. High OC concentrations occur in the urban areas with maximum concentrations of approximately 3–4 $\mu g\ m^{-3}$. In areas affected by wildfire, the maximum concentration is approximately 9 $\mu g\ m^{-3}$ as shown in Panel 7(a). As shown in Panels 7(b) and (c), maximum contributions from diesel and gasoline engines are approximately 0.36 and 0.55 $\mu g\ m^{-3}$, respectively. Wildfires generate a large amount of OC. The highest concentration of OC due to wildfire is approximately 8.32 $\mu g\ m^{-3}$ as shown in Panel 7(d). Panel 7(e) shows that open burning is an important source of OC with a highest average contribution of 1.25 $\mu g\ m^{-3}$. All other sources combined contribute to as high as 2.20 $\mu g\ m^{-3}$ of OC. The highest concentration occurs in industrial areas, further confirming that industrial sources account for the majority of the emissions from the "other" source category.

Fig. 8 shows the predicted episode-averaged source contribution to primary $PM_{2.5}$ mass concentrations. Panel 8(a) shows that primary $PM_{2.5}$ concentrations in the Houston urban and industrial areas are approximately 8–10 $\mu g\ m^{-3}$. The contribution due to upwind sources to primary $PM_{2.5}$ in the 4 km domain is approximately 1%. Highest contribution from diesel engines is approximately 1.6 $\mu g\ m^{-3}$. Contributions from diesel engines are higher than contributions from gasoline engines by approximately a factor of 2. High sulfur fuel contributes less than 0.8 $\mu g\ m^{-3}$ in both HGB and BPA areas. Contributions from wood smoke can be as high as 10 $\mu g\ m^{-3}$. Panel 8 (g) shows that open burning contributes to approximately 25% of the primary $PM_{2.5}$ in urban areas. Panel 8(h) illustrates that road dust contributes significantly to primary $PM_{2.5}$ especially in some rural areas north of Houston. The concentration can be as high as 2.52 $\mu g\ m^{-3}$. Analysis of the emissions inventory shows that unpaved road dust emissions account for over 95% of the road dust emissions. Other sources, mostly industrial sources, can contribute to approximately 4–6 $\mu g\ m^{-3}$ of primary $PM_{2.5}$. The contribution from sea salt is confined to the coastal areas and is small compared to other sources (see Fig. S11).

4.4. Source apportionment of secondary inorganic components

In previous receptor-oriented source apportionment studies, source contributions to sulfate were not determined because most of the sulfate is secondary. Buzcu et al. (2006) suggested that heterogeneous reactions of SO_2 on the surface of wood smoke particles could lead to increased sulfate concentrations in areas downwind of wildfires. In this study, we focus on understanding the sources of secondary sulfate from major SO_2 sources and the relative contributions from local (sources in the HGB and BPA areas) vs. upwind sources (sources located outside the 4 km domain) without considering the potential heterogeneous pathways.

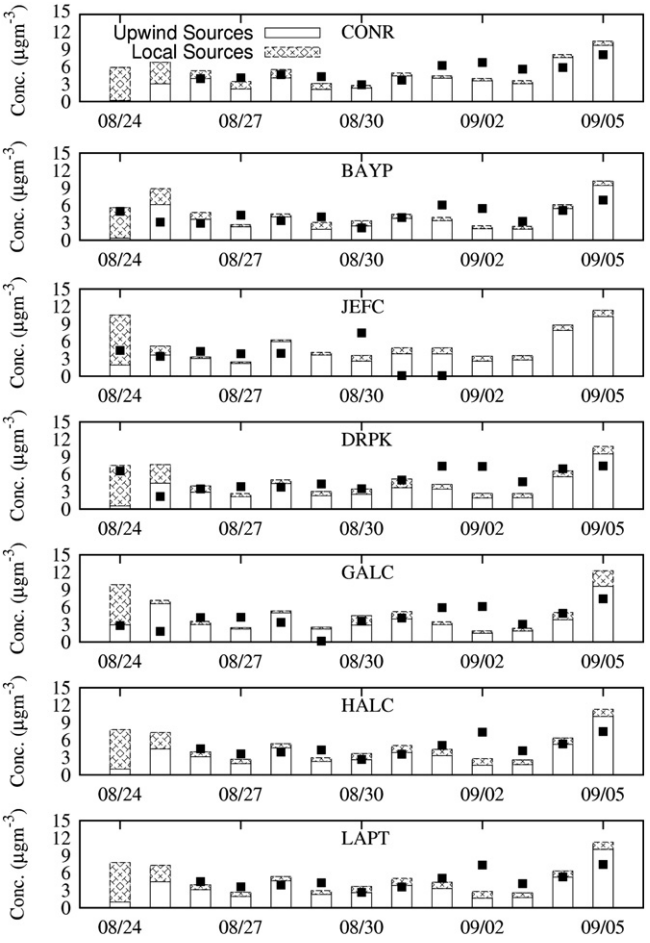

Fig. 9. Time series of 24-h averaged observed (closed rectangle) and predicted (stacked bars) $PM_{2.5}$ sulfate concentrations from sources within the 4 km domain (Local Sources) and upwind sources (Upwind Sources). Units are $\mu g\ m^{-3}$.

Fig. 9 shows the time series of predicted and observed 24-h averaged $PM_{2.5}$ sulfate concentrations at 7 observation sites. The predicted sulfate concentrations are broken down to show contributions from local sources and upwind sources. In the first two days, most of the sulfate in the domain is due to initial conditions and the contribution from upwind sources is small. In the rest of the days, predicted concentrations generally agree well with observations at all the sites and upwind sources dominate the sulfate concentration with relative contributions of more than 80% at most stations. Sulfate concentrations are under-predicted on September 1–2, 2000 at most stations in the HGB area, suggesting that a regional sulfate event was not captured by the model. Fig. S12 is a more detailed 1-h resolution time series that shows the major sources that contribute to the upwind sulfate are coal combustion and high sulfur fuel.

Fig. 10 shows the predicted regional contributions to 24-h averaged secondary $PM_{2.5}$ sulfate concentrations from different SO_2 sources on September 5, 2009, when the concentrations at all observation sites are highest throughout the simulated episode. The source contributions to $PM_{2.5}$ sulfate (Panel 10(a)) from primary emissions, upwind secondary sources and local sources of high sulfur fuel, coal combustion and other sources are shown on Panels 10(b)–(f), respectively. The overall sulfate concentration in HGB area is approximately 8–10 μg m^{-3}. Primary emissions can contribute to as high as 2.2 μg m^{-3} but the contributions from primary emissions to sulfate in HGB and BPA areas are less than 1 μg m^{-3}. Panel 10(c) shows that secondary sulfate from upwind sources accounts for almost all regional sulfate in the HGB and BPA areas. Local sources of SO_2 are not major sources of sulfate. SO_2 emitted from local sources of coal combustion contributes to a maximum of 1.8 μg m^{-3} on that day but most of the contributions are seen off the coast due to significant regional transport. Panels 10(g)–(i) illustrate the sources that contribute to the upwind secondary sulfate as shown in Panel 10(c). Coal combustion is the largest source with contributions of 5–7 μg m^{-3} and high sulfur fuel (mostly natural gas burning) is the second largest source with contributions of 3–4 μg m^{-3} in the HGB and BPA areas. All other sources combined only contribute to less than 1 μg m^{-3} in most part of the domain.

The low contributions from local SO_2 sources are expected since the reaction rate of SO_2 with hydroxyl radical (OH) is relatively slow as discussed in Buzcu et al. (2006). The half-life of SO_2 assuming a day time average OH concentration of 6×10^6 molecules cm^{-3} is on the order of 50 h at room temperature. Using a typical SO_2 concentration of 5 ppb and a reaction time of 10 h, it can be shown that only 1.5 μg m^{-3} sulfate can be formed. Thus, most of the sulfate observed in the HGB area should be from non-local sources. This analysis agrees with the more detailed model calculations shown in Fig. 10. It should be noted that the model calculation in this paper does not consider the potential heterogeneous pathways, which may lead to higher local source contributions. However, regional emissions control is necessary to significantly reduce the sulfate contributions in HGB and BPA areas.

Fig. 11 shows the regional distribution of 24-h averaged $PM_{2.5}$ ammonium ion concentrations and the major contributing sources on September 5, 2000. Since the PM emission profiles used in the emission processing do not include ammonium ion, the ammonium ion shown in Fig. 11 is entirely secondary. The maximum 24-h average $PM_{2.5}$ ammonium ion concentration is approximately 4 μg m^{-3}. Panel 11(b) shows an almost uniform regional background ammonium ion concentration of 0.05 μg m^{-3}. This regional background is due to the condensation of ammonia that enters the model simulation through the boundary condition specified for the 36 km parent domain. Panel 11(c) shows that the contribution of gasoline engines to ammonium ion is mostly located in urban areas with a maximum value of 1.1 μg m^{-3}. Most of the ammonia emissions are from catalyst-equipped light-duty gasoline vehicles (Kean et al., 2008). Contributions to ammonium ion due to diesel engines are small and not shown here. Contributions from oil/gas production and high sulfur fuel are generally small. The combined contributions from the two sources are approximately 0.14 μg m^{-3} as shown in Panel 11(d). Contribution from wildfires could reach

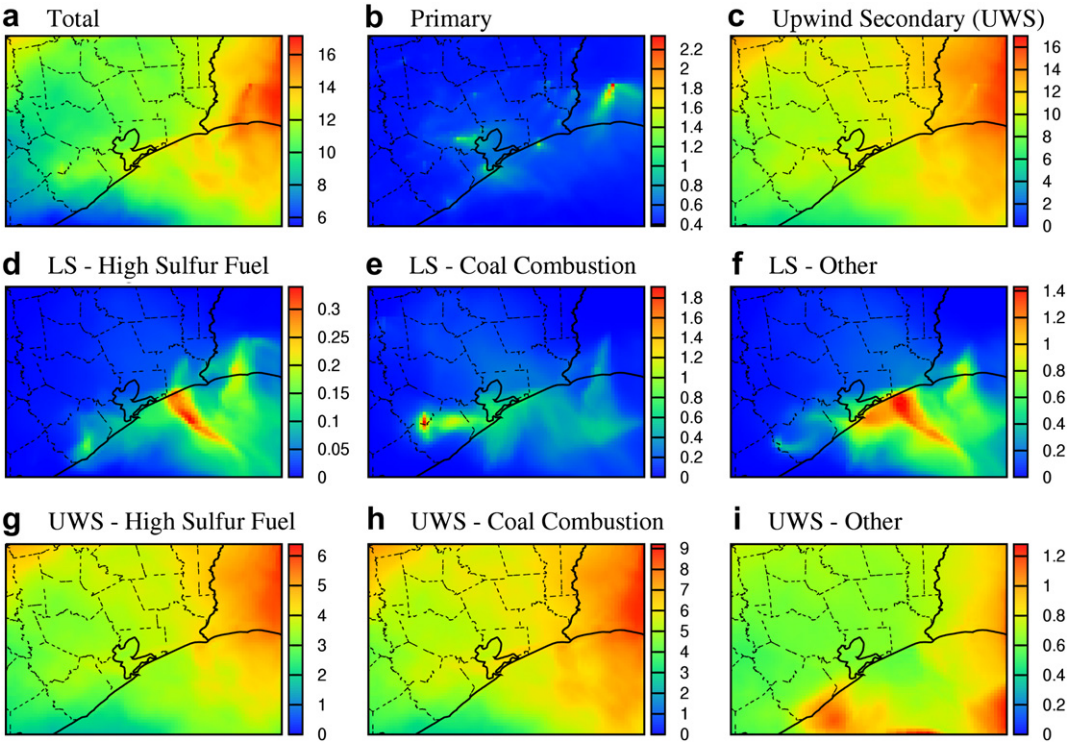

Fig. 10. Source apportionment of $PM_{2.5}$ sulfate concentrations on September 5, 2000. The scale on each panel is different. Units are μg m^{-3}.

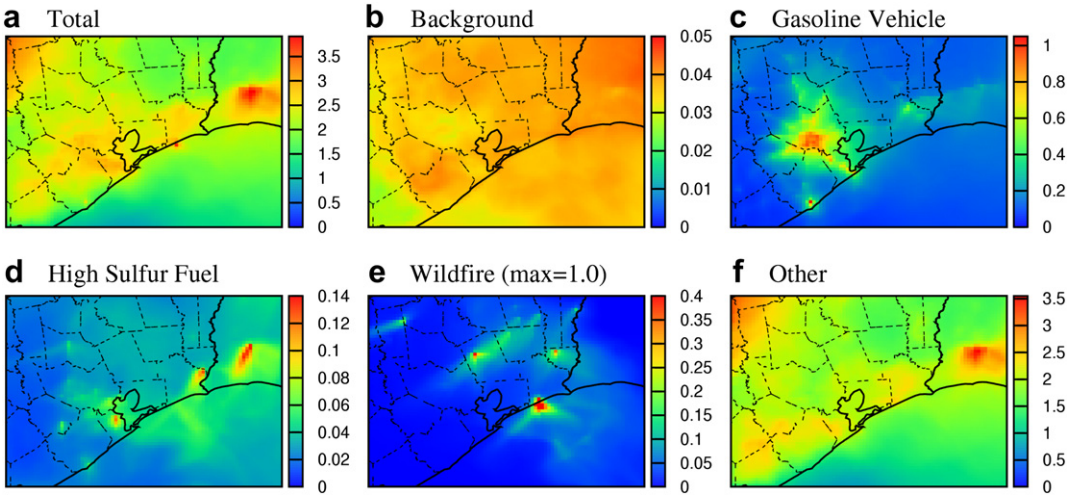

Fig. 11. Source apportionment of $PM_{2.5}$ ammonium ion concentrations on September 5, 2000. The scale on each panel is different. Units are $\mu g\ m^{-3}$. The scale of Panel (e) is adjusted to show better spatial distribution and the maximum value is shown with the title.

a maximum value of approximately 1 $\mu g\ m^{-3}$ in the vicinity of the fire. The majority of the ammonium ion is from the "other" sources category and is mainly due to gas-to-particle partitioning of ammonia emitted from agriculture sources, such as dairy operations and fertilizer applications.

5. Conclusions

The nested version of the source-oriented UCD/CIT model was used to simulate the source contributions to primary and secondary inorganic PM during the TexAQS 2000 in the HGB and BPA areas. The predicted concentrations of EC, OC, sulfate, ammonium ion and primary $PM_{2.5}$ mass generally agree with the filter-based observations as well as AMS analysis. Predicted source contributions to primary OC and $PM_{2.5}$ mass are also compared with a CMB model calculation. The UCD/CIT model, based on current emission inventory, shows PM emissions from sources other than diesel/gasoline vehicles and wood burning account for a significant fraction of primary OC and $PM_{2.5}$. Significant emissions of OC and $PM_{2.5}$ are from industrial sources and road construction based on the emission inventory data. This is not in agreement with the CMB results and implies that further investigations on the industrial and other PM emissions are necessary.

The UCD/CIT model predicts that EC was mainly from diesel engines. The majority of the primary OC was from internal combustion engines (diesel and gasoline engines) and industrial sources. Open burning was found to contribute large fractions of EC, OC and primary $PM_{2.5}$ mass in the HGB and BPA areas. Road dust, internal combustion engines and industrial sources were the major sources of primary $PM_{2.5}$. Wildfire dominated the contributions to all primary PM components and mass in areas near the fires. Secondary ammonium sulfate accounted for majority of the secondary inorganic PM. Over 80% of the secondary sulfate in the 4 km domain was produced in upwind areas. Coal combustion is largest source of sulfate. Ammonium ion was mainly agriculture sources and contributions from gasoline vehicles are predicted to be significant in urban areas.

Acknowledgement

This research is supported by funding from Texas Air Research Center under projects #077ATM0980A and #078ATM2080A, and from U.S EPA under grant #RD-83386501. The authors would also like to thank TCEQ for providing meteorology simulation results, Dr. David Allen for providing wildfire emissions and Drs. Jose-Luis Jimenez and Manjula Canagaratna for providing the AMS analysis data.

Appendix. Supplementary material

Supplementary data associated with this article can be found in the online version at doi:10.1016/j.atmosenv.2010.06.004.

References

Banta, R.M., Senff, C.J., Nielsen-Gammon, J., Darby, L.S., Ryerson, T.B., Alvarez, R.J., Sandberg, S.P., Williams, E.J., Trainer, M., 2005. A bad air day in Houston. Bulletin of the American Meteorological Society 86, 657–669.

Bhave, P.V., Pouliot, G.A., Zheng, M., 2007. Diagnostic model evaluation for carbonaceous $PM_{2.5}$ using organic markers measured in the southeastern US. Environmental Science & Technology 41, 1577–1583.

Boylan, J.W., Russell, A.G., 2006. PM and light extinction model performance metrics, goals, and criteria for three-dimensional air quality models. Atmospheric Environment 40, 4946–4959.

Bullock, K.R., Duvall, R.M., Norris, G.A., McDow, S.R., Hays, M.D., 2008. Evaluation of the CMB and PMF models using organic molecular markers in fine particulate matter collected during the Pittsburgh Air Quality Study. Atmospheric Environment 42, 6897–6904.

Buzcu, B., Yue, Z.W., Fraser, M.P., Nopmongcol, U., Allen, D.T., 2006. Secondary particle formation and evidence of heterogeneous chemistry during a wood smoke episode in Texas. Journal of Geophysical Research 111 (D10S13).

Byun, D., Ching, J., 1999. Science Algorithms of the EPA Models-3 Community Multiscale Air Quality Modeling System EPA/600/R-99/030. US Environmental Protection Agency, Office of Research and Development, Washington, DC.

Byun, D., Schere, K.L., 2006. Review of the governing equations, computational algorithms, and other components of the models-3 Community Multiscale Air Quality (CMAQ) modeling system. Applied Mechanics Reviews 59, 51–77.

Byun, D.W., Kim, S.T., Kim, S.B., 2007. Evaluation of air quality models for the simulation of a high ozone episode in the Houston metropolitan area. Atmospheric Environment 41, 837–853.

Carter, W.P.L., 1990. A detailed mechanism for the gas-phase atmospheric reactions of organic-compounds. Atmospheric Environment Part A – General Topics 24, 481–518.

Chen, J., Ying, Q., Kleeman, M.J., 2010. Source apportionment of wintertime secondary organic aerosol during the California regional $PM_{10}/PM_{2.5}$air quality study. Atmospheric Environment 44, 1331–1340.

Chen, J.J., Ying, Q., Kleeman, M.J., 2009. Source apportionment of visual impairment during the California regional $PM_{10}/PM_{2.5}$ air quality study. Atmospheric Environment 43, 6136–6144.

De Gouw, J.A., Hekkert, S.T.L., Mellqvist, J., Warneke, C., Atlas, E.L., Fehsenfeld, F.C., Fried, A., Frost, G.J., Harren, F.J.M., Holloway, J.S., Lefer, B., Lueb, R., Meagher, J.F., Parrish, D.D., Patel, M., Pope, L., Richter, D., Rivera, C., Ryerson, T.B., Samuelsson, J., Walega, J., Washenfelder, R.A., Weibring, P., Zhu, X., 2009.

Airborne measurements of ethene from industrial sources using laser photoacoustic spectroscopy. Environmental Science & Technology 43, 2437–2442.
Fraser, M.P., Yue, Z.W., Buzcu, B., 2003. Source apportionment of fine particulate matter in Houston, TX, using organic molecular markers. Atmospheric Environment 37, 2117–2123.
Fritz, S.G., 2000. Locomotive Fuel Effects Study: Particulate Size Characterization. Final Report. Southwest Research Institute.
Gong, S.L., Barrie, L.A., Blanchet, J.P., von Salzen, K., Lohmann, U., Lesins, G., Spacek, L., Zhang, L.M., Girard, E., Lin, H., Leaitch, R., Leighton, H., Chylek, P., Huang, P., 2003. Ganadian aerosol module: a size-segregated simulation of atmospheric aerosol processes for climate and air quality models – 1. Module development. Journal of Geophysical Research – Atmospheres 108.
Hays, M.D., Fine, P.M., Geron, C.D., Kleeman, M.J., Gullett, B.K., 2005. Open burning of agricultural biomass: physical and chemical properties of particle-phase emissions. Atmospheric Environment 39, 6747–6764.
Kean, A.J., Littlejohn, D., Ban-Weiss, G.A., Harley, R.A., Kirchstetter, T.W., Lunden, M. M., 2008. Trends in on-road vehicle emissions of ammonia. Atmospheric Environment 43, 1565–1570.
Kleeman, M.J., Cass, G.R., 2001. A 3d Eulerian source-oriented model for an externally mixed aerosol. Environmental Science & Technology 35, 4834.
Kleeman, M.J., Cass, G.R., Eldering, A., 1997. Modeling the airborne particle complex as a source-oriented external mixture. Journal of Geophysical Research 102, 21355–21372.
Kleeman, M.J., Schauer, J.J., Cass, G.R., 1999. Size and composition distribution of fine particulate matter emitted from wood burning, meat charbroiling, and cigarettes. Environmental Science & Technology 33, 3516–3523.
Kleeman, M.J., Schauer, J.J., Cass, G.R., 2000. Size and composition distribution of fine particulate matter emitted from motor vehicles. Environmental Science & Technology 34, 1132–1142.
Kleeman, M.J., Ying, Q., Lu, J., Mysliwiec, M.J., Griffin, R.J., Chen, J.J., Clegg, S., 2007. Source apportionment of secondary organic aerosol during a severe photochemical smog episode. Atmospheric Environment 41, 576–591.
Kleinman, L.I., Daum, P.H., Imre, D., Lee, Y.-N., Nunnermacker, L.J., Springston, S.R., Weinstein-Lloyd, J., Rudolph, J., 2002. Ozone production rate and hydrocarbon reactivity in 5 urban areas: a cause of high ozone concentration in Houston. Geophysical Research Letters 29, 105.
Kupiainen, K.J., Tervahattu, H., Raisanen, M., Makela, T., Aurela, M., Hillamo, R., 2005. Size and composition of airborne particles from pavement wear, tires, and traction sanding. Environmental Science & Technology 39, 699–706.
Lane, T.E., Pinder, R.W., Shrivastava, M., Robinson, A.L., Pandis, S.N., 2007. Source contributions to primary organic aerosol: comparison of the results of a source-resolved model and the chemical mass balance approach. Atmospheric Environment 41, 3758–3776.
Lewis, E.R., Schwartz, S.E., 2006. Comment on "size distribution of sea-salt emissions as a function of relative humidity". Atmospheric Environment 40, 588–590.
Nam, J., Kimura, Y., Vizuete, W., Murphy, C., Allen, D.T., 2006. Modeling the impacts of emission events on ozone formation in Houston, Texas. Atmospheric Environment 40, 5329–5341.
Nopmongcol, U., Khamwichit, W., Fraser, M.P., Allen, D.T., 2007. Estimates of heterogeneous formation of secondary organic aerosol during a wood smoke episode in Houston, Texas. Atmospheric Environment 41, 3057–3070.
Robinson, A.L., Subramanian, R., Donahue, N.M., Bernardo-Bricker, A., Rogge, W.F., 2006. Source apportionment of molecular markers and organic aerosols. 3. Food cooking emissions. Environmental Science & Technology 40, 7820–7827.
Schauer, J.J., Cass, G.R., 2000. Source apportionment of wintertime gas-phase and particle-phase air pollutants using organic compounds as tracers. Environmental Science & Technology 34.
Sweeten, J.M., Parnell, C.B., Shaw, B.W., Auvermann, B.W., 1998. Particle size distribution of cattle feedlot dust emission. Transactions of the ASAE 41, 1477–1481.
Taback, H.J., Brienza, A.R., Marko, J., Brunetz, N., 1979. Fine Particulate Emissions from Stationary and Miscellaneous Sources in the South Coast Air Basin. California Air Resources Board, Sacramento, California.
Vizuete, W., Kim, B.U., Jeffries, H., Kimura, Y., Allen, D.T., Kioumourtzoglou, M. A., Biton, L., Hendersona, B., 2008. Modeling ozone formation from industrial emission events in Houston, Texas. Atmospheric Environment 42, 7641–7650.
Vukovich, J.M., Pierce, T., 2002. The Implementation of BEIS3 within the SMOKE Modeling Framework. MCNC-Environmental Modeling Center , Research Triangle Park and National Oceanic and Atmospheric Administration.
Wagstrom, K.M., Pandis, S.N., Yarwood, G., Wilson, G.M., Morris, R.E., 2008. Development and application of a computationally efficient particulate matter apportionment algorithm in a three-dimensional chemical transport model. Atmospheric Environment 42, 5650–5659.
Wang, C.F., Chang, C.Y., Tsai, S.F., Chiang, H.L., 2005. Characteristics of road dust from different sampling sites in northern Taiwan. Journal of the Air & Waste Management Association 55, 1236–1244.
Watson, J.G., Zhu, T., Chow, J.C., Engelbrecht, J., Fujita, E.M., Wilson, W.E., 2002. Receptor modeling application framework for particle source apportionment. Chemosphere 49, 1093–1136.
Wert, B.P., Trainer, M., Fried, A., Ryerson, T.B., Henry, B., Potter, W., Angevine, W.M., Atlas, E., Donnelly, S.G., Fehsenfeld, F.C., Frost, G.J., Goldan, P.D., Hansel, A., Holloway, J.S., Hubler, G., Kuster, W.C., Nicks, D.K., Neuman, J.A., Parrish, D.D., Schauffler, S., Stutz, J., Sueper, D.T., Wiedinmyer, C., Wisthaler, A., 2003. Signatures of terminal alkene oxidation in airborne formaldehyde measurements during TexAQS 2000. Journal of Geophysical Research – Atmospheres 108.
Wood, E.C., Canagaratna, M.R., Herndon, S.C., Kroll, J.H., Onasch, T.B., Kolb, C.E., Worsnop, D.R., Knighton, W.B., Seila, R., Zavala, M., Molina, L.T., DeCarlo, P.F., Jimenez, J.L., Weinheimer, A.J., Knapp, D.J., Jobson, B.T., Stutz, J., Kuster, W.C., Williams, E.J., 2010. Investigation of the correlation between odd oxygen and secondary organic aerosol in Mexico City and Houston. Atmospheric Chemistry and Physics Discussion 10, 3547–3604.
Ying, Q., Kleeman, M.J., 2006. Source contributions to the regional distribution of secondary particulate matter in California. Atmospheric Environment 40, 736–752.
Ying, Q., Lu, J., Allen, P., Livingstone, P., Kaduwela, A., Kleeman, M.J., 2008a. Modeling air quality during the California Regional $PM_{10}/PM_{2.5}$ Air Quality Study (CRPAQS) using the UCD/CIT source-oriented air quality model – part I. Base case model results. Atmospheric Environment 42, 8954–8966.
Ying, Q., Lu, J., Kaduwela, A., Kleeman, M.J., 2008b. Modeling air quality during the California Regional $PM_{10}/PM_{2.5}$ Air Quality Study (CRPAQS) using the UCD/CIT source-oriented air quality model – part II. Regional source apportionment of primary airborne particulate matter. Atmospheric Environment 42, 8967–8978.
Ying, Q., Krishnan, A., 2010. Source contributions of volatile organic compounds to ozone formation in Southeast Texas. Journal of Geophysical Research-Atmospheres, in press, 10.1029/2010JD013931.
Ying, Q., Lu, J., Kleeman, M.J., 2009. Modeling air quality during the California Regional $PM_{10}/PM_{2.5}$ Air Quality Study (CRPAQS) using the UCD/CIT source oriented air quality model – part III. Regional source apportionment of secondary and total airborne particulate matter. Atmospheric Environment 43, 419–430.
Zhang, K.M., Knipping, E.M., Wexler, A.S., Bhave, P.V., Tonnesen, G.S., 2005a. Size distribution of sea-salt emissions as a function of relative humidity. Atmospheric Environment 39, 3373–3379.
Zhang, L.M., Gong, S.L., Padro, J., Barrie, L.A., 2001. A size-segregated particle dry deposition scheme for an atmospheric aerosol module. Atmospheric Environment 35, 549–560.
Zhang, Q., Alfarra, M.R., Worsnop, D.R., Allan, J.D., Coe, H., Canagaratna, M.R., Jimenez, J.L., 2005b. Deconvolution and quantification of hydrocarbon-like and oxygenated organic aerosols based on aerosol mass spectrometry. Environmental Science & Technology 39, 4938–4952.
Zheng, M., Cass, G.R., Schauer, J.J., Edgerton, E.S., 2002. Source apportionment of $PM_{2.5}$ in the Southeastern United States using solvent-extractable organic compounds as tracers. Environmental Science & Technology 36, 2361–2371.